RSC Advances

REVIEW

View Article Online
View Journal | View Issue

Cite this: *RSC Adv.*, 2022, **12**, 181

Modification of carbon-based nanomaterials by polyglycerol: recent advances and applications

Zeinab Rafiee[a] and Sakineh Omidi *[b]

Received 12th October 2021
Accepted 7th December 2021

DOI: 10.1039/d1ra07554c

rsc.li/rsc-advances

Hyperbranched polymers, a subclass of dendritic polymers, mimic nature's components such as trees and nerves. Hyperbranched polyglycerol (HPG) is a hyperbranched polyether with outstanding physicochemical properties, including high water-solubility and functionality, biocompatibility, and an antifouling feature. HPG has attracted great interest in the modification of different objects, in particular carbon-based nanomaterials. In this review, recent advances in the synthesis and application of HPG to modify carbon-based nanomaterials, including graphene, carbon nanotubes, fullerene, nanodiamonds, carbon dots, and carbon fibers, are reviewed.

1. Introduction

Recently, much attention has been paid to synthesizing carbon-based nanomaterials which are dispersible in organic solvents and aqueous media.[1–3] So, the functionalization of carbon materials has been widely performed by a broad range of dendritic polymers.[4–6] Polyglycerol (PG), polyethyleneimine (PEI), polycaprolactone (PCL), polylactic acid (PLA), and (PAMAM) are the most useful dendritic polymers for the functionalization of carbon-based nanomaterials. Among these polymers, hyperbranched polyglycerol (HPG) has had a great influence, specifically in biomedical applications due to its numerous advantages such as dendritic structure, high solubility, chemical stability, low toxicity, low/absent immunogenicity, and excellent biocompatibility.[7–11]

HPG involves a random branch-on-branch structure with a large number of functional hydroxyl groups in their branches, which make it completely soluble in water. HPG shows the combined features and advantages of linear and dendritic polymers. HPG, as a hydrophilic polymer, has recently attracted a lot of attention for improving the water-solubility of hydrophobic drugs such as curcumin.[12] The other remarkable properties of HPG are availability, low viscosity, commercial viability, and abundant reactive hydroxyl groups.[13] HPG can be prepared in a single-step reaction and straightforward synthesis with high yields. The first polymerization of glycidol was reported by Sandler *et al.* in 1966.[14] After that, the cationic ring-opening polymerization method was introduced. This method was initiated by Lewis or Brønsted acids with two mechanisms, with an active chain end or an activated monomer.[15,16] The uncontrolled synthesis of the hyperbranched polymer is the main disadvantage of cationic ring-opening polymerization. To overcome this problem, the anionic ring-opening multi-branching polymerization of glycidol has been substituted. This method involves the growth of HPG on the surface of a core, acting as the initiator in the polymerization process. In this method, glycidol is added drop-wise to the deprotonated core, and the temperature is gradually increased.[17–19] In rare cases, HPG was synthesized by the polymerization of monomers other than glycidol.[20] In recent years, Adeli and coworkers have reported the polymerization of glycidol at room temperature by citric acid[21] and ascorbic acid[22] as the initiators. Citric acid and ascorbic acid are the proton donors and can activate the cationic ring-opening polymerization of glycidol under ambient conditions.

Although the production of HPG with a high molecular weight up to 1000 kDa is possible,[23] high molecular weight polymers are not suitable for biomedical applications because they are not biodegradable and accumulate in different organs.[24] To improve biodegradability, different acid-sensitive moieties were randomly incorporated into the backbone of HPG.[25] Some degradable moieties, including acid-sensitive ketal, acetal, ester, and disulfide linkages, gave the same result regarding their biodegradability features.[26–28] These studies showed that the kind of degradable linkages make a direct impression on the hydrolytic half-life and consequently on the *in vivo* properties of the biodegradable HPG.

One of the outstanding features of HPG is the versatility of its structure and properties through manipulation of its functional groups.[20,29,30] This strategy is the main approach for designing appropriate systems for different biomedical applications. Zhao *et al.* showed greater hydrophilicity for HPG than for polyethylene glycol (PEG) by significantly improving the dispersion of superparamagnetic iron oxide particles in the aqueous phase.[31] PEG is of primary interest in the fabrication of drug formulations, in particular, the coating of cancer drugs. The

[a]*Department of Chemistry, Malayer University, Malayer, Iran*
[b]*Shahid Beheshti University of Medical Sciences, Tehran, Iran. E-mail: sakineh.omidi@yahoo.com; Tel: +98-9181438542*

coupling of PEG to drugs reduces non-specific protein adsorption and the tendency of particles to aggregate. Therefore, PEGylated formulations show high stability, efficiency, and biocompatibility.[32] Despite these advantages, PEG is a linear polymer with two functional hydroxyl groups at the end, which limits the further modification of the formulation with targeting moieties. HPG can be an attractive alternative for PEG owing to the presence of a greater number of hydroxyl groups that provide potential sites for the modification and conjugation of bioactive agents and targeting moieties. Also, compared to PEG, HPG is more hydrophilic and covers a larger surface area because of its hyperbranched structure.[33] Several review articles have been published on the synthesis and various applications of HPG in recent years.[34–38]

Nanomaterials have gained significant research interest due to their novel physicochemical properties, such as unique shape and size, and mechanical, thermal, and optical properties, as well as their high surface area. Among the various nanomaterials, carbon-based nanomaterials, such as graphene, carbon nanotubes, fullerene, and nanodiamonds, are ideal precursors for use in various fields, particularly in the fabrication of biomaterials, drug delivery systems (DDSs), and cancer diagnostic and therapeutic applications.[39,40] Owing to the intrinsic hydrophobic nature of carbon-based nanomaterials, it seems that their combination with hydrophilic polymers such as HPG will have benefits. In this review, we focus on modifying carbon-based nanomaterials, including graphene, carbon nanotubes, fullerene, nanodiamonds, carbon dots, and carbon fibers by HPG, as well as their various applications in recent studies.

2. Graphene

Graphene is two-dimensional (2D) monolayers of carbon and has been given a lot consideration due to its unique properties, including large surface area and chemical stability. Graphene-based materials have been used in various fields, such as energy storage,[41] antibacterial agents,[42] cancer treatment,[43] and sensors.[44] Despite their potent medical properties, the use of graphene-based materials has been hindered by their low dispersibility in aqueous solutions. In 2010 for the first time, to improve their thermal stability and water-dispersibility, covalent functionalization of graphene oxide with polyglycerol was applied for anchoring magnetic nanoparticles (NPs). For this purpose, Fe–Au NPs were functionalized with 4-mercaptophenylboronic acid through well-developed Au–S chemistry and then grafted onto the surface of PG by boroester bonds. The nanohybrid structures were able to form a stable dispersion in water.[45] In 2015 Cai *et al.* used a facile process for the covalent functionalization of surface graphene with HPG *via* the epoxy ring-opening polymerization of glycidol. The outstanding aim of this work was attributed to the promotion of the dispersion and hydrophilicity of the resultant nanomaterials.[46]

2.1. HPG-graphene platforms in drug delivery

Cancer is one of the most common causes of death worldwide, and chemotherapy plays a significant role in its treatment. The major challenges in using anticancer drugs such as doxorubicin (DOX) are low bioavailability, drug-resistance, and serious side effects.[47] In this regard, the development of DDSs based on 2D nanomaterials such as graphene is a good strategy for overcoming these limitations. Adeli's research team reported the edge-functionalization of graphene by attaching polyglycerol with a bi-dentate naphthol segment. The hydrophobicity of the flat surface and the hydrophilicity of the functionalized edges led to the formation of a nanocapsule system with a hydrophobic core and a hydrophilic shell. The synthesized supramolecule was stable in aqueous solutions and able to encapsulate hydrophobic DOX with a high capacity.[48] A few years later, this research team developed a hybrid of graphene and polyglycerol with curcumin (nrGO–PG-Cur) for photothermal therapeutics by near-infrared (NIR) laser irradiation.[49] They showed that the amount of polyglycerol could affect the system stability and drug release. The results of 3-(4,5-dimethylthiazolyl-2)-2,5-diphenyltetrazolium bromide (MTT) and apoptosis assays indicated that the release of the drug in phosphate buffer saline (PBS) increased up to 5-fold when nrGO–PG-Cur was exposed to NIR laser irradiation. They also showed that functionalized graphene sheets with HPG are resistant to nonspecific interactions with bovine serum albumin (BSA), which is a valuable property for biomedical applications. The structural defects of the graphene sheets obtained by this method were minimized, and dispersed graphene showed a high photothermal conversion capacity.[50]

In 2017, modified graphene oxide (GO) with HPG was synthesized *via* an anionic ring-opening polymerization method to deliver DOX to tumor cells.[51] The synthesized HPG-GO indicated good stability in aqueous solution, a high loading capacity for DOX, and good blood compatibility with negligible effect on hemolysis or blood coagulation. There was no significant histological difference between the HPG-GO group and the PBS control group, which is attributed to the good biocompatibility of HPG-GO as verified through histological analysis. The non-toxicity of HPG-GO could be a result of its characteristic chemical structure as well as the biocompatible nature of HPG and GO. Haag and Adeli's research team functionalized the surface of nanographene sheets-HPG with triphenylphosphonium (TPP) and 2,3-dimethyl maleic anhydride (DA). TPP is a mitochondrial targeting ligand, and conjugation with DA causes a charge conversion from negative to positive upon decreasing the pH from 7.4 to 6.8, which facilitates cellular uptake. The nanosystem showed a high loading capacity for DOX, selective drug delivery, and good photothermal properties upon NIR irradiation.[52]

In 2018, a modified GO with HPG (HPG-GO) was applied to load quercetin, a hydrophobic anticancer drug, through non-covalent interactions. Grafting with HPG creates an expanded distance between GO nanosheets, and drug molecules are physically entrapped in the cavities between branches of the polymer. For comparison with HPG-GO, grafted linear polypropylene oxide on GO (PPO-GO) was also used to load and release the drug. The results showed a more sustained and controllable release behavior from HPG-GO. The drug-loading capacity of HPG-GO was approximately five times that of PPO-

GO.[53] In an attractive study, mesoporous silica-coated magnetic graphene oxide (Fe_3O_4-GO-mSiO_2) was entirely covered by polyglycerol-*g*-polycaprolactone to study the biodegradability, controlled release, and pH-sensitive behavior of the DOX-loaded formulation. Arraying Fe_3O_4 NPs on graphene oxide sheets provides the required magnetic property for DDSs. DOX loading on this formulation resulted from electrostatic interactions in mesoporous silica and supramolecular π–π stacking with GO sheets. The DOX release increased from 61% to 86% with a decrease in pH from 7.4 to 5.5, which can result from the reduction in hydrophobic and electrostatic interactions of DOX with GO sheets and mesoporous silica. Moreover, polymer grafting on Fe_3O_4-GO-mSiO_2 plays a vital role in the controllable DOX release process.[54] Pourjavadi *et al.* synthesized the nanocarrier rGO-PCH-p-Hyd-*g*-HPG by grafting HPG on poly(epichlorohydrin)-functionalized GO and replacing chlorine groups in the main-chain with hydrazine groups. Doxorubicin and curcumin were attached to the carrier by forming a hydrazone bond and π–π stacking interactions, respectively. The resulting DDS showed a pH-sensitive release behavior and a synergistic effect against MCF-7 cancer cells because of an improvement in the cellular uptake of drugs.[55]

2.2. HPG-graphene platforms as catalysts

There have been only a few reports in the catalyst field for HPG in recent years,[56] but catalytic chemistry is an important application of graphene-based materials. In 2018, Cu(II) immobilized on HPG-GO was used as an efficient and reusable catalyst to synthesize aminonaphthoquinone derivatives.[57] In another study, sulfonated GO-HPG was used as a nontoxic acid catalyst to synthesize benzo[*a*]pyrano-[2,3-*c*] phenazine derivatives under solvent-free conditions[58] and ultrasound irradiation.[59] A high yield of products was obtained under both conditions, although ultrasonic irradiation significantly reduced the reaction time. Naeimi and coworkers designed a heterogeneous catalyst by immobilization of Cu(II) on hyperbranched polyglycerol functionalized graphene oxide (GO-HPG-IA-Cu(II)) for the synthesis of naphthoquinone derivatives.[60]

2.3. HPG-graphene platforms as virus and bacteria inhibitors

The search for new routes to combat viruses and bacteria is a crucial global health challenge. In recent years, polyglycerol-functionalized graphene has been proposed to develop virus and bacteria inhibitors. Haag and coworkers, in a valuable piece of research, synthesized a 2D polymer structure *via* the functionalization of GO with sulfated dendritic polyglycerol by a grafting approach. The resultant nanostructures were a mimic of heparin and showed potent inhibitory action against viruses. The robust interactions with the viral membrane proteins were supported by negatively charged sulfate groups on the surface of the 2D nanosystems.[61] This research team showed that graphene scaffolds offered a developed surface area to increase the volume of the polyglycerol sulfate group. Also, they proved that the inhibitory efficacy is controlled by the size of the polymeric nanomaterials and the degree of sulfation. The best inhibiting graphene sheets were about 300 nm in size and had a degree of sulfation of about 10%.[62] Adeli, Haag, and coworkers proposed a controlled covalent functionalization method for graphene sheets by a one-pot nitrene [2 + 1] cycloaddition reaction with 2,4,6-trichloro-1,3,5-triazine, sodium azide, and thermally reduced graphene oxide under mild conditions to generate defined bifunctional 2D nanomaterials. This method was further proved by the stepwise attachment of several functionalized macromolecules, such as azido-polyglycerol ($HPGN_3$), polyglycerol amine (HPG-NH_2), and amino-β-cyclodextrin (β-CD-NH_2).[63] Haag's research team, using a pericyclic [2 + 1] cycloaddition reaction, prepared a functionalized thermally reduced graphene oxide (TRGO) with dendritic polyglycerol (dPG) azide and linear polyglycerol (lPG) azide to investigate their inhibition effect against two types of enveloped viruses. 2D hybrid derivatives showed strong inhibitory effects equal to or better than the commonly used standards of heparin or enrofloxacin.[64] In 2017, this research team reported the controlled functionalization of graphene sheets by conjugating dichlorotriazine on the surface of graphene and subsequent conversion of chloro groups to HPG and polyglycerol sulfate. Polysulfated nanomaterials can mimic the extracellular cell matrix. Polysulfated graphene derivatives with control over their functionality are valuable for obtaining highly effective 2D platforms for pathogen interactions. A highly sulfated 2D material could trap 20 virions and showed IC_{50} values as low as 5.7 ± 2.1 μg mL^{-1}, which is better than for nonsulfated analogs.[65] In another study, alkyl amines with various chain lengths (6, 9, 10, 11, and 12 carbon atoms) were attached to graphene–polyglycerol sulfate, and G–PGS–C*x* (x = 6, 9, 10, 11, and 12) were produced. The interactions of G–PGS–C*x* with virions of feline coronavirus (FCoV) and SARS-CoV-2, the cause of COVID-19, were investigated. The G–PGS–C*x* platforms with long aliphatic chains (≥10) indicated stronger inhibition of both coronaviruses. G–PGS–C11, without significant toxicity against human cells, was the most potent antiviral agent against FCoV and SARS-CoV-2 with IC_{50} values of 6.3 ± 1.2 μg mL^{-1} and 0.8 ± 0.3 2 μg mL^{-1}, respectively. The negatively charged PGS interacted with the positively charged surface of the virion; then the long aliphatic chains were able to diffuse into the cellular membrane and induce cell death.[66] Recently, Adeli and Haag's team used graphene as a template to synthesize 2D polyglycerols. HPG was conjugated to the surface of graphene *via* pH-sensitive linkers. Then polyglycerol units were crosslinked in two dimensions through a click reaction. The produced 2D polyglycerol nanosheets were unfastened from the graphene platform by slight acidification and were sulfated to form sulfate proteoglycans 2D-hPGS as mimics of heparin (Fig. 1). The ability of 2D-hPGS and their three-dimensional (3D) analogs (3D-hPGS) for virus inhibition was investigated. 2D-hPGS showed strong inhibition of infection with an IC_{50} of 20 μg mL^{-1} against HSV-1, while the value of IC_{50} for 3D-HPGS was four times higher than that of 2D-hPGS. These results exhibited the critical role of topology in virus inhibition. 2D-hPGS have a higher surface area than their 3D analogs and interact more efficiently with HS-binding domains on the surface of the virus. In contrast, a lot of

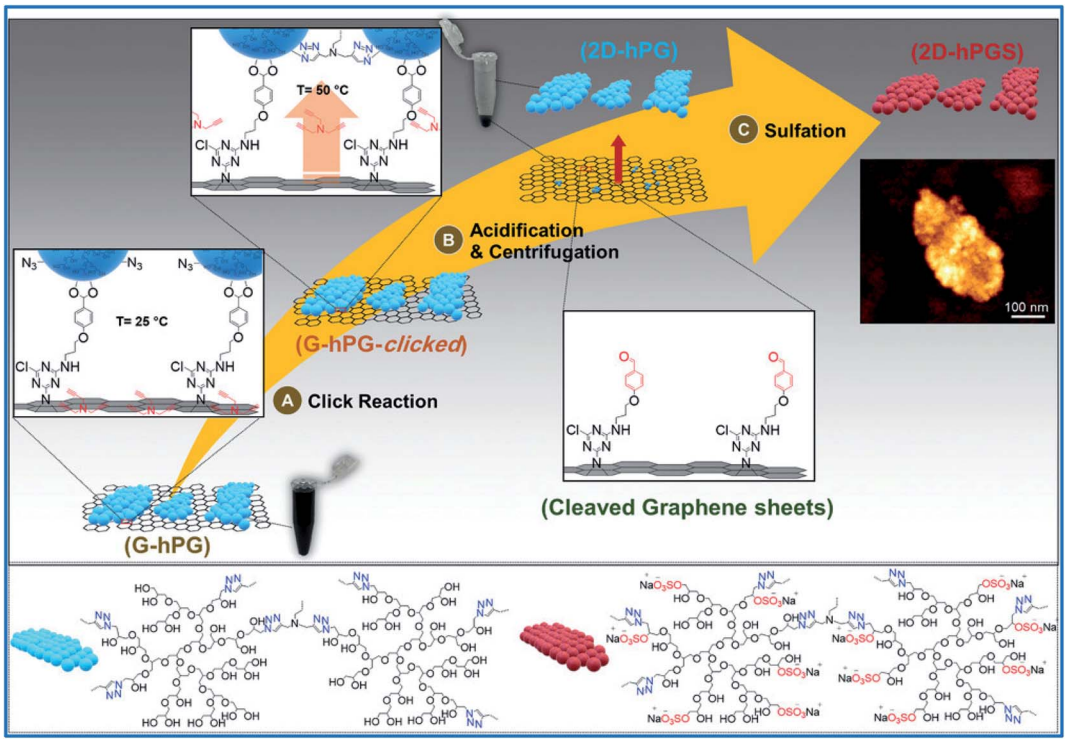

Fig. 1 Schematic representation of the synthesis procedure for 2D hyperbranched polyglycerol. Finally, 2D polyglycerol remains in the supernatant upon centrifugation. The inset shows an SFM image of the final multivalent 2D-hPGS nanosheets. Reprinted from ref. 67 with permission from John Wiley and Sons.

sulfate groups of 3D-hPGS are not available for interaction with virions.[67]

Two cytotoxicity mechanisms, "trapping" and "nano-knives", have been proposed for the antibacterial activity of graphene-based materials. Adeli and Haag's research team synthesized graphene sheets functionalized by polyglycerol (TRGO-PG) with a neutral surface, polyglycerol sulfate (TRGO-PGS) with a negative surface, polyglycerol amine (TRGO-PGA) with a positive surface, and zwitterionic graphene nanomaterials (ZGNMs), with both polyglycerol sulfate and polyglycerol amine. The authors used these 2D nanomaterials to investigate the validity of the "trapping" and "nano-knife" mechanisms. *Escherichia coli* (*E. coli*) bacteria showed a considerable binding adhesion force only with TRGO-PGA, since *E. coli* and the TRGO-PGA sheets were negatively and positively charged, respectively. The polymer-functionalized graphene sheets, regardless of surface charge or concentration, did not show any harmful activity against Gram-positive or Gram-negative bacteria. In contrast, the functionalized graphene sheets without polymer coverage ($TRGO-NH_2$) showed concentration-dependent antibacterial activity against both *E. coli* and *Bacillus cereus* bacteria. These results demonstrated that the availability of the basal plane and edges of the graphene sheets is necessary for their antibacterial activity. In polyglycerol-functionalized graphene materials, the polymer branches cover the basal plane and edges of the graphene sheets and hinder their interactions with pathogens.[68]

2.4. Other applications of HPG-graphene platforms

HPG-functionalized graphene oxide and HPG-modified superparamagnetic iron oxide nanoparticles were covalently bonded together to form an adsorbent to remove the antibiotic tetracycline from aqueous solution. The adsorbent showed excellent dispersibility and an adsorption capacity of 684.93 mg g^{-1} at 298 K.[69] Rezaeifar *et al.* modified the surface of GO using HPG *via* direct polycondensation by thionyl chloride. The sorbent capability of the synthesized nanocomposite was considered by a hollow fiber solid/liquid microextraction technique to extract and determine ibuprofen and naproxen as target compounds in hair and wastewater.[70] These authors also applied the synthesized HPG-GO to provide an electrochemical sensor to detect flutamide in a human plasma sample. The voltammetry assays showed that the constructed electrochemical sensor was reproducible and sensitive.[71] Flutamide is a widely used antiandrogen and anticancer drug for the treatment of prostate cancer. Lee *et al.* polymerized the glycidol at the hydroxyl groups on the GO surface, followed by esterification with butyric anhydride. The synthesized HGO dispersed in the poly(vinyl chloride) (PVC) matrix to form a series of PVC/HGO nanocomposite films with improved mechanical strength, durability, and gas barrier properties.[72]

3. Carbon nanotubes (CNTs)

Carbon nanotubes (CNTs), an allotrope of carbon, have great potential in various fields, such as biomedicine, but poor

solubility and biological toxicity have limited their applications.[73] Modification of CNTs by various polymers such as HPG could be an appropriate approach. Adeli *et al.* grafted HPG onto multi-wall carbon nanotubes (MWCNTs) and reported the low cytotoxicity of the resultant MWCNT-*g*-PG.[74] Shortly afterwards, the same authors showed that PG grafting onto the surface of CNTs changes the extended conformation of the hybrid towards a closed state, and this conformation can encapsulate small hydrophobic molecules such as ferrocene. The hydroxyl end functional groups of PG and their noncovalent interactions, including hydrogen bonding, were recognized as being responsible for the changes in the conformation of MWCNTs.[75]

3.1. HPG-CNT platforms in drug delivery

Zhou *et al.* prepared a macroinitiator of hydroxyl-functionalized multiwalled carbon nanotubes (MWNT-OH) by one-pot nitrene chemistry. Then, HPG was covalently grafted onto the surfaces of MWNT-OH by a grafting technique. Rhodamine 6B fluorescent molecules were conjugated to the surface of MWNT-*g*-HPG *via* frequent functional hydroxyl groups of HPG to prepare a promising nanohybrid in the drug delivery, cell imaging, and bioprobing fields.[76] Huang *et al.* modified carbon nanotubes with HPG through host–guest interactions.[77] For this purpose, they synthesized β-cyclodextrin-HPG (β-CD-HPG) *via* anionic polymerization. CNTs with hydroxyl groups were synthesized and combined with 1,1-adamantanecarbonyl chloride to form CNT-Ad. The supramolecular host–guest interaction between β-CD-HPG and CNT-Ad led to the formation of CNT-β-CD-HPG composites that revealed excellent water-dispersibility and great potential for controlled cancer drug delivery (Fig. 2). In 2019, folic acid was grafted onto the surface of HPG-modified MWCNTs (MWNTs-$_{OX}$-PG) to obtain a targeted drug delivery system MWNTs-$_{OX}$-PG-COOH-FA. The nanosystem could form a good dispersion for 48 h in physiological environments.[78]

3.2. Other applications of HPG-CNT platforms

In 2017, Ernst *et al.* synthesized the amphiphilic molecule PerPG including a hydrophilic polyglycerol dendron, perylene-derived dye core, and alkyl chain parts.[79] PerPG was used for the noncovalent functionalization of a carbon nanotube. The polyglycerol dendron offered water-solubility and biocompatibility to the nanotube, and the perylene-derived dye core enabled noncovalent attachment to the nanotube through π–π stacking. An MTT assay indicated that the nanotube–PerPG complex is biocompatible at concentrations related to biotechnological applications. In an interesting study, a layer of hyperbranched polyglycerol sulfate (HPGS) homogenously covered the CNT *via* sonication. HPGS-dispersed CNTs were coated onto electrospun polycaprolactone fiber to achieve nanostructured fibrous scaffolds PCL-CNT-HPGS. The fabricated scaffolds, due to the high surface area-to-volume ratios, can promote the adhesion and proliferation of induced pluripotent stem (IPS) cells and induce longer axons and higher neural differentiation efficiency compared to bare PCL fibers. Since the neurites follow the path of the fiber scaffolds, the aligned PCL-CNT-HPGS guide the arrangement of generated neurites. The length of neurites grown on aligned fibers can reach 752 μm.[80]

4. Fullerene

Fullerenes and their derivatives have various applications in biomedical science as antioxidants, antivirals, and anticancer agents.[81] Covalent and noncovalent functionalization of

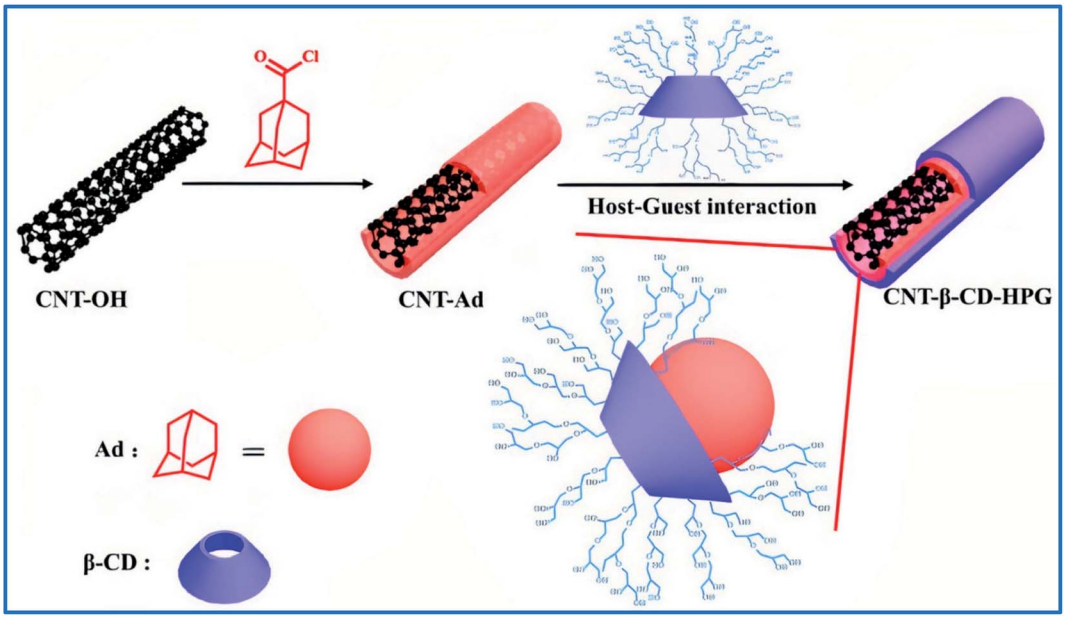

Fig. 2 Preparation of CNT-β-CD-HPG that relies on host–guest interaction between β-CD and Ad. (Ad: adamantanecarbonyl). Reprinted from ref. 77 with permission from Elsevier.

fullerene by HPG improves its applicability. Eskandar *et al.* used β-CD-HPG to produce water-soluble fullerene.[82] They investigated the host–guest interactions between β-CD-HPG and fullerene C_{60} with 1 : 1 and 1 : 2 stoichiometries, and showed that the complex was formed in the most stable 1 : 2 stoichiometric ratio. C_{60}-based water-soluble materials can contribute to advances in medical chemistry and different biological fields. In 2016, Beiranvand *et al.* used the [2 + 1] nitrene cycloaddition reaction to obtain triazine-functionalized fullerene (Full-Trz).[83] Full-Trz showed great fluorescence emission, and it was used in bioimaging. HPG with amino functional groups was attached to Full-Trz *via* a nucleophilic reaction at the triazine group to increase its poor water-solubility.

4.1. HPG-fullerene platforms in drug delivery

Adeli and coworkers used fullerene C_{60} as a macroinitiator for the anionic polymerization of glycidol and prepared fullerene-HPG amphiphiles (FPAs). These nanohybrids could self-assemble controllably into crosslinked nanoclusters, and were able to transport hydrophobic and hydrophilic guest molecules.[84] A little later, the authors showed that the number of polyglycerol branches, adjusted by the amount of *t*-BuO^-K^+ used in the synthesis, affects the aggregation size of various FPAs in aqueous solutions, loading capacity, and the release of encapsulated hydrophobic dyes, but not their cellular uptake. Dye-labelled derivatives of FPAs as a probe in the study of cellular uptake showed that FPAs could transfer small molecules into cells *via* endocytotic pathways. Low toxicity, biocompatibility, and water-solubility introduce the FPAs nanocarriers as favorable candidates for drug delivery.[85] Also, a thermodynamic study showed that a fullerene-HPG nanostructure with sodium citrate forms aqueous biphasic systems (ABS) in aqueous media. ABS can be used to separate biomolecules such as cells, proteins, nucleic acids, and enzymes in a low-cost and high-yield process.[86]

4.2. HPG-fullerene platforms as virus inhibitors

In 2018, Adeli and coworkers, using a sulfur trioxide pyridine complex, reported a sulfation reaction on FPA and synthesized fullerene-polyglycerol sulfates (FPS). Investigation of the interaction of FPS with cellular and viral proteins showed that the sulfate groups at the branches and fullerene core are essential for binding to proteins and the infection inhibition of vesicular stomatitis virus (VSV).[87]

5. Nanodiamonds

Diamond nanoparticles, called nanodiamonds (NDs), due to the unique characteristics of diamonds and the intrinsic properties of nanometer-sized particles, have attracted increasing attention in recent years. Fluorescent nanodiamonds act as nanoscale thermometers on the surface of HPG-gold NPs, which is beneficial for photothermal therapy.[88] In 2011, Komatsu and coworkers synthesized ND derivatives with increased solubility by HPG (Fig. 3). They had previously synthesized functionalized ND-PEG, but its solubility was not adequate for biomedical applications.[89] The prepared ND-PG showed extremely high solubility in buffer solutions.[90] In addition to increasing solubility, compared to PEG grafting, it has been shown that coating with ND or superparamagnetic iron oxide nanoparticles (SPION) with PG creates more resistance to protein adsorption and a resulting avoidance of macrophage uptake.[91] On the other hand, functionalization of ND-PG with carboxyl and amino group and the formation of positively and negatively charged nanoparticles resulted in exclusive adsorption to the proteins of opposite charges.[92]

5.1. HPG-ND platforms in drug and gene delivery

In 2014, Komatsu's group used ND-PG as a drug carrier platform for cancer therapy. To evade non-specific cell uptake and achieve high targeting efficacy, the cyclic Arg-Gly-Asp (RGD) peptide was grafted to ND-PG. RGD peptide can specifically bind to the receptors of tumor tissue cells. Cisplatin and DOX anticancer drugs were loaded on the PG, and the cellular uptake of the obtained ND-PG-RGD-Pt[93] and dND-PG-RGD-DOX[94] showed that the conjugated nanoparticles show cytotoxicity only against cancer cells and not healthy cells due to the targeting effect of RGD as well as the stealth effect of PG. Zhao, Chen *et al.* evaluated dND-PG-RGD-DOX (nano-DOX) to treat the deadly brain tumor glioblastoma (GBM). They showed that nano-DOX induces an anti-cancer immunogenic cell death

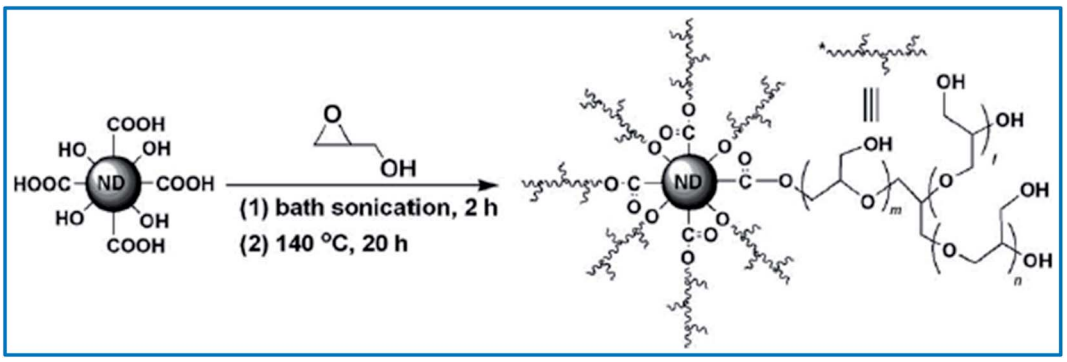

Fig. 3 Synthesis of ND functionalized with hyperbranched polyglycerol through the ring-opening polymerization of glycidol. Reprinted from ref. 90 with permission from John Wiley and Sons.

(ICD) response in GBM.[95,96] In addition, nano-DOX can suppress the transcription factor STAT3, which is the activator of many actions, including apoptosis inhibition in GBM.[97] In another study, this research team indicated that nano-DOX acts by different mechanisms from free DOX on human glioblastoma cells (GC). While DOX-treated GC showed signs of apoptosis, nano-DOX activated autophagy and stimulated the expression and release of HMGB1, which is a prominent member of damage-associated molecular patterns (DAMPs). HMGB1 protected GC against apoptosis.[98] Indeed they showed that nano-DOX has a reduced therapeutic potency compared to free DOX. The reduced killing potency caused lower toxicity to non-malignant tissues and evasion of the multidrug resistance (MDR) phenomenon, which is a significant problem in chemotherapy by DOX.[99] In addition to DOX, Zhao and Komatsu prepared ND-PG conjugated with Cyanine (ND-PG-Cy7).[100] ND-PG-Cy7 with long half-life blood circulation, owing to the stealth effect of PG, accumulated in the tumor which can lead to clear fluorescence images. For a similar purpose, to utilize the intrinsic fluorescence of nanodiamonds, Torelli and coworkers prepared fluorescent nanodiamonds (FNDs) with a polyglycerol shell (FND-PG).[101] For targeted tumor imaging, FND-PG was conjugated to several copies of the single-chain version of vascular endothelial growth factor (VEGF), which is associated with angiogenesis in a growing tumor.

Komatsu *et al.* presented gene delivery systems by click conjugation of ND-PG-N_3 and some polypeptides terminated with propargyl glycine. The systems had high positive zeta potentials demonstrating their potential ability for gene delivery.[102] Later, the authors used a similar process for the functionalization of mesoporous bioactive glass (MBG)[103] and TiO_2 nanoparticles[104] instead of ND. The synthesized nanosystems indicated high efficiency for gene delivery and biomedical applications, respectively. Also, ND-PG-N_3 was used to prepare ND-PG-gadolinium(III), termed ND-PG-Gd(III), with high dispersibility and stability in PBS.[105] Earlier, it was found that ND-Gd(III) conjugates are promising contrast agents for magnetic resonance imaging (MRI), but suffered from poor dispersibility in physiological media.[106] Komatsu and coworkers, in addition to various hydrophilic NDs mentioned above, synthesized hydrophobic NDs by etherification of ND-PG with octyl and tetradecyl chains, which showed high dispersibility in chloroform.[107]

Haag and coworkers reported two core–shell nanoparticles with a PG shell and soft dendritic polyethylene or hard nanodiamond as the carbon cores.[108] For the two nanoparticles, the encapsulation capacities and transportability into tumor cells were compared with two model dyes. The results showed that the flexible core (dendritic polyethylene) plays a major role in the encapsulation/transport properties of the hydrophobic guest.

In addition to modifying carbon nanotubes by HPG,[77] Huang *et al.* also modified nanodiamonds with HPG through host–guest interactions.[109] Adamantine-functionalized ND (ND-Ad) and β-CD-HPG formed ND-β-CD-HPG composites. The potential of the new nanohybrid in drug delivery was explored by the loading and release of the anticancer agent DOX. The results showed a high drug-loading capability and controlled drug release behavior. The capacity of DOX loading on ND-β-CD-HPG was around 15.47 mg g^{-1} and the maximal release of DOX was at pH = 5.5 (37.8%) compared to pH = 7.4 (16.7%).

5.2. Other applications of HPG-ND platforms

Boudou *et al.* functionalized a fluorescent nanodiamond with HPG. The resulting nanoparticles could form a good dispersion in an aqueous, physiological medium and cultured cells, while the unique optical properties of the original fluorescent nanodiamond were preserved. Also, the abundant hydroxyl end-groups of HPG were used for covalent conjugation of nanoparticles to bovine serum albumin as a model protein.[110] In 2015, Cai *et al.* synthesized ND functionalized with HPG and used the synthesized ND-PG and poly(vinyl alcohol) (PVA) to prepare composite nanofibers by an electrospinning method.[111] The mechanical properties of the obtained nanofibers were improved, attributed to the abundant hydroxyl groups of PG, which led to better dispersion of nanofillers within the composite matrix and enhanced filler–matrix interactions. A nanocomposite of ND-PG and Fe_3O_4-PG was prepared, and the enzyme horseradish peroxidase (HRP) was immobilized on the PG layer. The nanocomposite was used as a biological catalyst for phenol biodegradation and showed better stability and catalytic activities than the free enzyme.[112]

6. Carbon dots

Carbon dots (CDs), of sizes of less than 10 nm, have been synthesized in a one-step procedure from various organic compounds *via* microwave or hydrothermal methods and usually have some biomedical applications, such as bioimaging, disease diagnosis, and nanoprobing.[113] The functionalization of CDs by neutral functional groups, such as hydroxyl groups instead of charged functional groups, is highly effective at avoiding complicated interactions with biomacromolecules and cells in biomedical applications. Li *et al.* synthesized CDs from α-cyclodextrin by hydrothermal carbonization and modified them with HPG to achieve advantages including biocompatibility, multifunctionality, low cytotoxicity, and good solubility. The resultant CDs-*g*-HPG showed high green fluorescence and could be a favorable nanostructure for bioimaging.[114] In another study, CDs were synthesized from citric acid and functionalized with HPG. The prepared nanomaterial showed high water-solubility with strong blue fluorescence.[115]

CDs are usable as fluorescence imagers and detectors for biological species due to their valuable optical properties. Zhao and coworkers separately grafted PG onto the surface of CDs and iron oxide nanoparticles (IOs) and then functionalized them with carboxyl and amino groups, respectively. The obtained materials were linked *via* an amide linkage to form an IO–PG–CD nanohybrid (Fig. 4). Cisplatin anticancer drug was loaded on the IO–PG–CD through complexation and investigated for delivery into tumor cells *in vitro*. IOs were used as a magnetically targeted DDS and showed a high improved anticancer efficacy *in vivo*.[116]

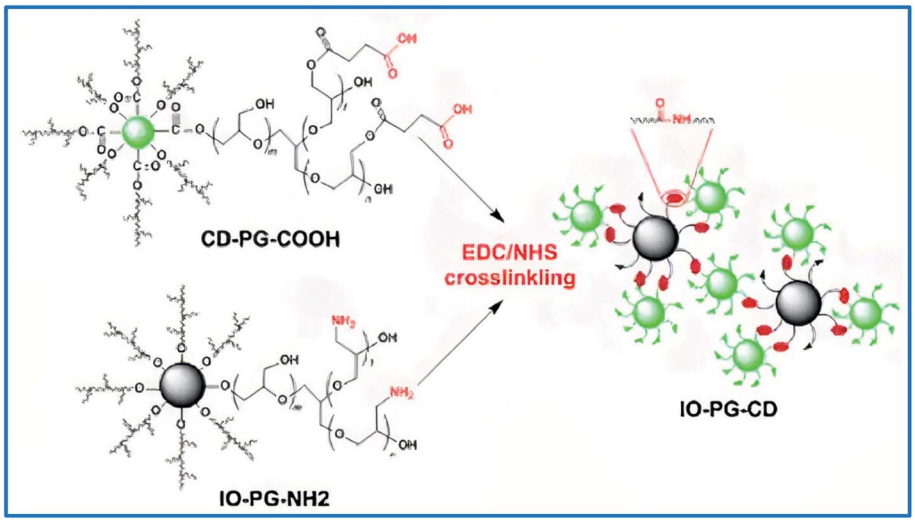

Fig. 4 Schematic representation of the IO–PG–CD nanohybrid through surface engineering of CDs and IOs and following EDC/NHS cross-linking. Reprinted from ref. 116 with permission from Elsevier.

In 2018, Cai *et al.* used PG-grafted SPION (SPION-PG) as the shell and PG-grafted mesoporous carbon nanoparticles (MCN-PG) as the core to prepare suitable MMCN nanocomposites for water purification. The presence of SPION in the nanohybrid made magnetic separation possible for removing and recycling an adsorbent using an external magnetic field. The nanocomposites showed a high adsorption capacity to remove methylene blue (MB) dye from aqueous media.[117]

7. Carbon fibers

Carbon fibers (CF), owing to their excellent mechanical properties, temperature tolerance, and light weight, have come to be ideal materials for employment in various fields, such as aerospace, performance carbon composites, and transporter applications.[118] To achieve improved mechanical properties and reinforced carbon fiber composites, Gao *et al.* grafted HPG and hyperbranched poly (amide amine) (HPAMAM) onto the carbon fiber surface. The presence of abundant functional groups improved the interfacial strength of the fiber-matrix; HPAMAM with amino groups was more efficient in advancing the interfacial properties of the fiber-matrix.[119] Also, an improvement in mechanical parameters was observed when HPG-grafted carbon fibers were used as the reinforcing phases in blend composites of the dicyanate ester of bisphenol-A (DCBA) and bisphenol-A based benzoxazine (BA-a) resins.[120] In 2017, Zhang and Shao's research team immobilized initiator groups onto the fiber surface *via* a two-step reaction. Then, HPG was grown on the CF by grafting polymerized glycidol (Fig. 5).[121] The size of the grafted HPG can be adjusted by this polymerization method.

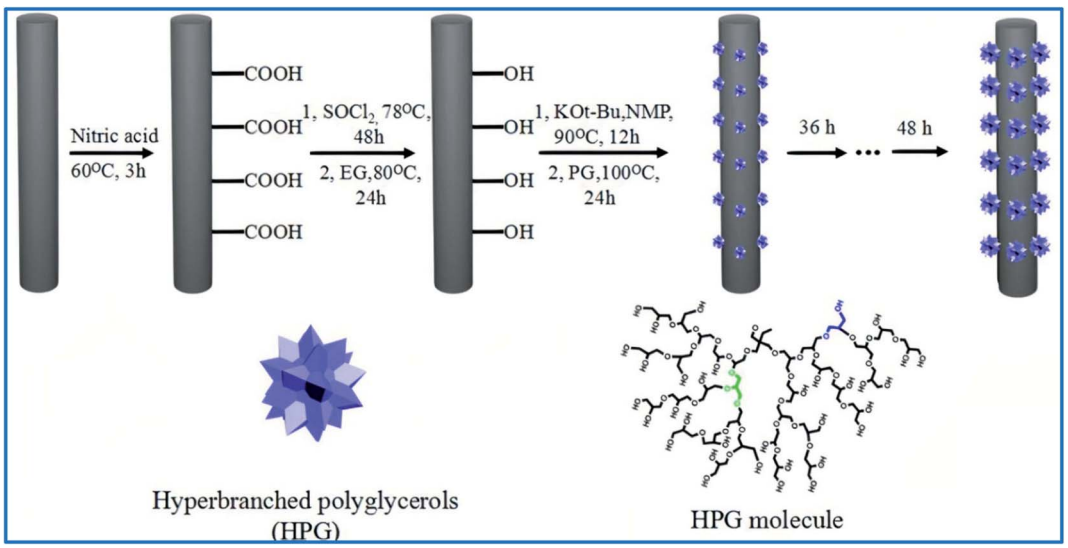

Fig. 5 The functionalized progress of carbon fibers by HPG. Reprinted from ref. 121 with permission from Elsevier.

Investigation of CF-HPG showed that its physicochemical properties, such as the interfacial strength between the fiber and the epoxy resin were improved, especially when the reaction time lasted for 48 hours. HPG also provided the functional groups for new designs and fabrication of carbon fiber composites.

8. Summary and future perspectives

A rising interest has been taken in recent years in the versatile applications of carbon-based materials, including graphene, CNTs, fullerenes, nanodiamonds, carbon dots, and carbon fibers. Modification of carbon nanomaterials with polymers can improve their efficiency in different fields, particularly biomedical applications. Graphene has received more attention than other carbon-based nanomaterials for modification by HPG. HPG-graphene platforms are used in various applications, including delivery of cancer drugs, virus and bacteria inhibition, and catalytic properties. Conjugation of HPG to graphene was performed *via* a covalent approach except for three cases,[48–50] in which the authors used strong noncovalent interactions between graphene and naphthol rings in the polyglycerol structure. Functionalization of graphene by HPG leads to the production of thermally-stable and water-dispersible nanomaterials. The delivery of anticancer drugs, including DOX,[48,51,52,54,55] curcumin,[49,55] and quercetin,[53] was the main application of HPG-graphene nanomaterials. The 2D structure of graphene provides a high loading capacity for drugs. On the other hand, grafting of a polymer to graphene creates an expanded distance between GO nanosheets and drug molecules physically entrapped in the cavities between the branches of the HPG. Also, HPG-graphene platforms showed a sustained release of anticancer drugs. The controlled release of curcumin was reported with NIR laser irradiation.[49] Functionalization of DDSs by targeting ligands is a main method for targeted drug delivery. In this case, only Haag *et al.* have used this method and functionalized nanographene sheets-HPG with the mitochondrial targeting ligand TPP. The designed nanosystem showed selective delivery and facilitated the cellular uptake of DOX.[52]

By functionalization of the hydroxyl groups of HPG-graphene platforms with various groups such as sulfonic acid and isatoic anhydride, efficient and reusable catalysts were obtained.[57–60] The catalytic applications have been studied only for graphene modified by HPG, which can be attributed to the large surface area and low cost of graphene compared to other carbon-based nanomaterials.

In a series of studies,[61,62,64–66] Haag's research team showed that functionalization of GO with a sulfated dendritic HPG can lead to the production of a mimic of heparin with the ability to inhibit viruses. Unlike antiviral properties, functionalization of graphene with HPG covers the edges and basal plane of graphene sheets and hinders the operation of "trapping" and "nano-knife" mechanisms, which are the main proposed mechanisms for the antibacterial activity of graphene-based materials.[68]

For the first time, HPG-modified NDs were synthesized by Komatsu *et al.* to increase the solubility of NDs for biomedical applications. The preparation of nanosystems for the delivery of anticancer drugs such as cisplatin[93] and DOX[94–99,109] is the main usage of HPG-ND conjugates. The nano-DOX obtained by Zhao and Chen's research team showed promising results for treating the brain tumor glioblastoma.[95–98] Also, the intrinsic fluorescence of nanodiamonds can be used to obtain clear fluorescence images.[101]

HPG was grafted onto the surfaces of CNTs *via* both covalent and noncovalent approaches. The noncovalent forces included host–guest interactions,[77] π–π stacking,[79] and multiple interactions (hydrogen bonds, van der Waal's forces, and H–π stacking interactions).[80] In addition to increasing solubility, polyglycerol bonding can decrease the cytotoxicity of CNTs. HPG-modified CNTs were suitable for DDSs,[74–78] biomedical applications,[79] and biocompatible platforms.[80]

HPG were conjugated to fullerene by covalent[83–87] and noncovalent[82] approaches to improve its water-solubility and biocompatibility. Grafting of HPG on the surface of carbon dots and carbon fibers were performed only by a covalent approach. Due to the inherent fluorescent property of carbon dots, HPG-modified carbon dots showed high water-solubility and a strong ability for bioimaging applications.[114–116] HPG-grafting can also improve the physicochemical properties of carbon fibers.[119–121]

In summary, this review provides a brief overview of recent HPG-modified carbon nanomaterials and their interesting applications in many fields, such as biomedicine, imaging, diagnosis, cancer therapy, and drug or gene delivery. The solubility of carbon nanomaterials has significantly increased *via* functionalization by HPG either by covalent or noncovalent approaches. In addition to increasing solubility, HPG offers other advantages, such as increased blood circulation time, biocompatibility, and low toxicity to hybrids.

It is suggested for future studies that different functional groups or targeting agents such as folic acid should be attached onto the surface of HPG. Also, resultant multifunctional HPGs should be further investigated for *in vitro* toxicity and preclinical *in vivo* studies to develop new formulations. Currently, the synthesis and applications of HPG are growing fast, and we believe that the broader use of HPG will be attainable in the near future.

Conflicts of interest

There are no conflicts to declare.

References

1 A. B. Bourlinos, V. Georgakilas, V. Tzitzios, N. Boukos, R. Herrera and E. P. Giannelis, *Small*, 2006, **2**, 1188–1191.
2 D. Konios, M. M. Stylianakis, E. Stratakis and E. Kymakis, *J. Colloid Interface Sci.*, 2014, **430**, 108–112.
3 A. O. Borode, N. A. Ahmed and P. A. Olubambi, *Phys. Fluids*, 2019, **31**, 071301.
4 J. Che, W. Yuan, G. Jiang, J. Dai, S. Y. Lim and M. B. Chan-Park, *Chem. Mater.*, 2009, **21**, 1471–1479.

5 N. G. Sahoo, S. Rana, J. W. Cho, L. Li and S. H. Chan, *Prog. Polym. Sci.*, 2010, **35**, 837–867.
6 V. D. Punetha, S. Rana, H. J. Yoo, A. Chaurasia, J. T. McLeskey Jr, M. S. Ramasamy, N. G. Sahoo and J. W. Cho, *Prog. Polym. Sci.*, 2017, **67**, 1–47.
7 R. K. Kainthan and D. E. Brooks, *Biomaterials*, 2007, **28**, 4779–4787.
8 S. Omidi, Z. Rafiee and A. Kakanejadifard, *Bioorg. Chem.*, 2021, 105308.
9 R. K. Kainthan, J. Janzen, J. N. Kizhakkedathu, D. V. Devine and D. E. Brooks, *Biomaterials*, 2008, **29**, 1693–1704.
10 M. Hu, M. Chen, G. Li, Y. Pang, D. Wang, J. Wu, F. Qiu, X. Zhu and J. Sun, *Biomacromolecules*, 2012, **13**, 3552–3561.
11 R. K. Kainthan, M. Gnanamani, M. Ganguli, T. Ghosh, D. E. Brooks, S. Maiti and J. N. Kizhakkedathu, *Biomaterials*, 2006, **27**, 5377–5390.
12 S. Omidi, Z. Rafiee and A. Kakanejadifard, *Bioorg. Chem.*, 2021, **116**, 105308.
13 H. Gheybi, S. Sattari, A. Bodaghi, K. Soleimani, A. Dadkhah and M. Adeli, in *Engineering of Biomaterials for Drug Delivery Systems*, Elsevier, 2018, pp. 103–171.
14 S. R. Sandler and F. R. Berg, *J. Polym. Sci., Part A-1: Polym. Chem.*, 1966, **4**, 1253–1259.
15 R. Tokar, P. Kubisa, S. Penczek and A. Dworak, *Macromolecules*, 1994, **27**, 320–322.
16 A. Dworak, W. Walach and B. Trzebicka, *Macromol. Chem. Phys.*, 1995, **196**, 1963–1970.
17 A. Sunder, R. Hanselmann, H. Frey and R. Mülhaupt, *Macromolecules*, 1999, **32**, 4240–4246.
18 A. Sunder, R. Mülhaupt, R. Haag and H. Frey, *Adv. Mater.*, 2000, **12**, 235–239.
19 M. Ilg and J. Plank, *Ind. Eng. Chem. Res.*, 2019, **58**, 12913–12926.
20 P. G. Parzuchowski, A. Świderska, M. Roguszewska, T. Frączkowski and M. Tryznowski, *Polymer*, 2018, **151**, 250–260.
21 E. Mohammadifar, A. Bodaghi, A. Dadkhahtehrani, A. Nemati Kharat, M. Adeli and R. Haag, *ACS Macro Lett.*, 2017, **6**, 35–40.
22 M. Dadkhah, H. Shamlooei, E. Mohammadifar and M. Adeli, *RSC Adv.*, 2018, **8**, 217–221.
23 R. K. Kainthan, E. B. Muliawan, S. G. Hatzikiriakos and D. E. Brooks, *Macromolecules*, 2006, **39**, 7708–7717.
24 B. D. Ulery, L. S. Nair and C. T. Laurencin, *JJ. Polym. Sci., Part B: Polym. Phys.*, 2011, **49**, 832–864.
25 R. A. Shenoi, J. K. Narayanannair, J. L. Hamilton, B. F. Lai, S. Horte, R. K. Kainthan, J. P. Varghese, K. G. Rajeev, M. Manoharan and J. N. Kizhakkedathu, *J. Am. Chem. Soc.*, 2012, **134**, 14945–14957.
26 R. A. Shenoi, B. F. Lai and J. N. Kizhakkedathu, *Biomacromolecules*, 2012, **13**, 3018–3030.
27 R. A. Shenoi, B. F. Lai, M. Imran ul-haq, D. E. Brooks and J. N. Kizhakkedathu, *Biomaterials*, 2013, **34**, 6068–6081.
28 R. A. Shenoi, S. Abbina and J. N. Kizhakkedathu, *Biomacromolecules*, 2016, **17**, 3683–3693.
29 M. Quadir, S. Fehse, G. Multhaup and R. Haag, *Molecules*, 2018, **23**, 1281.
30 A. Utrata-Wesołek, W. Wałach, M. Bochenek, B. Trzebicka, J. Anioł, A. L. Sieroń, J. Kubacki and A. Dworak, *Eur. Polym. J.*, 2018, **105**, 313–322.
31 L. Zhao, T. Chano, S. Morikawa, Y. Saito, A. Shiino, S. Shimizu, T. Maeda, T. Irie, S. Aonuma and H. Okabe, *Adv. Funct. Mater.*, 2012, **22**, 5107–5117.
32 N. A. Alcantar, E. S. Aydil and J. N. Israelachvili, *J. Biomed. Mater. Res.*, 2000, **51**, 343–351.
33 A. S. A. Lila, K. Nawata, T. Shimizu, T. Ishida and H. Kiwada, *International journal of pharmaceutics*, 2013, **456**, 235–242.
34 S. Abbina, S. Vappala, P. Kumar, E. M. Siren, C. C. La, U. Abbasi, D. E. Brooks and J. N. Kizhakkedathu, *J. Mater. Chem. B*, 2017, **5**, 9249–9277.
35 S. I. Bhat, Y. Ahmadi and S. Ahmad, *Ind. Eng. Chem. Res.*, 2018, **57**, 10754–10785.
36 N. Rades, K. Licha and R. Haag, *Polymers*, 2018, **10**, 595.
37 M. Jafari, S. S. Abolmaali, H. Najafi and A. M. Tamaddon, *Int. J. Pharm.*, 2020, **576**, 118959.
38 M. Rahman, M. Alrobaian, W. H. Almalki, M. H. Mahnashi, B. A. Alyami, A. O. Alqarni, Y. S. Alqahtani, K. S. Alharbi, A. Fransis and A. Hafeez, *Drug Discovery Today*, 2020, **26**, 1006–1017.
39 M. Sajjadi, M. Nasrollahzadeh, B. Jaleh, G. J. Soufi and S. Iravani, *J. Drug Targeting*, 2021, 1–26.
40 D. Maiti, X. Tong, X. Mou and K. Yang, *Front. Pharmacol.*, 2019, **9**, 1401.
41 A. Olabi, M. A. Abdelkareem, T. Wilberforce and E. T. Sayed, *Renewable Sustainable Energy Rev.*, 2021, **135**, 110026.
42 S. Omidi, A. Kakanejadifard and F. Azarbani, *J. Iran. Chem. Soc.*, 2018, **15**, 1467–1475.
43 H. Sharma and S. Mondal, *Int. J. Mol. Sci.*, 2020, **21**, 6280.
44 X. Jin, C. Feng, D. Ponnamma, Z. Yi, J. Parameswaranpillai, S. Thomas and N. Salim, *Chemical Engineering Journal Advances*, 2020, 100034.
45 T. A. Pham, N. A. Kumar and Y. T. Jeong, *Synth. Met.*, 2010, **160**, 2028–2036.
46 N. Cai, D. Hou, L. Shen, X. Luo, Y. Xue and F. Yu, *Funct. Mater. Lett.*, 2015, **8**, 1550068.
47 X.-J. Liang, C. Chen, Y. Zhao and P. C. Wang, in *Multi-Drug Resistance in Cancer*, Springer, 2010, pp. 467–488.
48 S. Movahedi, M. Adeli, A. K. Fard, M. Maleki, M. Sadeghizadeh and F. Bani, *Polymer*, 2013, **54**, 2917–2925.
49 F. Bani, M. Adeli, S. Movahedi and M. Sadeghizadeh, *RSC Adv.*, 2016, **6**, 61141–61149.
50 F. Bani, A. Bodaghi, A. Dadkhah, S. Movahedi, N. Bodaghabadi, M. Sadeghizadeh and M. Adeli, *Lasers in Medical Science*, 2018, **33**, 795–802.
51 S. Mu, G. Li, Y. Liang, T. Wu and D. Ma, *Mater. Sci. Eng., C*, 2017, **78**, 639–646.
52 Z. Tu, H. Qiao, Y. Yan, G. Guday, W. Chen, M. Adeli and R. Haag, *Angew. Chem.*, 2018, **130**, 11368–11372.
53 M. Islami, A. Zarrabi, S. Tada, M. Kawamoto, T. Isoshima and Y. Ito, *Int. J. Nanomed.*, 2018, **13**, 6059.
54 A. Pourjavadi, Z. M. Tehrani and S. Jokar, *J. Ind. Eng. Chem.*, 2015, **28**, 45–53.
55 A. Pourjavadi, S. Asgari and S. H. Hosseini, *J. Drug Delivery Sci. Technol.*, 2020, **56**, 101542.

56 J. Anjali and K. Sreekumar, *Catal. Lett.*, 2019, **149**, 1952–1964.
57 H. Naeimi and M. F. Zarabi, *Tetrahedron*, 2018, **74**, 2314–2323.
58 H. Naeimi and M. F. Zarabi, *RSC Adv.*, 2019, **9**, 7400–7410.
59 M. F. Zarabi and H. Naeimi, *Polycyclic Aromat. Compd.*, 2019, **39**, 1–20.
60 H. Naeimi and M. Farahnak Zarabi, *Can. J. Chem.*, 2019, **97**, 728–736.
61 B. Ziem, H. Thien, K. Achazi, C. Yue, D. Stern, K. Silberreis, M. F. Gholami, F. Beckert, D. Gröger and R. Mülhaupt, *Adv. Healthcare Mater.*, 2016, **5**, 2922–2930.
62 B. Ziem, W. Azab, M. Gholami, J. P. Rabe, N. Osterrieder and R. Haag, *Nanoscale*, 2017, **9**, 3774–3783.
63 A. Faghani, I. S. Donskyi, M. Fardin Gholami, B. Ziem, A. Lippitz, W. E. Unger, C. Böttcher, J. P. Rabe, R. Haag and M. Adeli, *Angew. Chem.*, 2017, **129**, 2719–2723.
64 B. Ziem, J. Rahn, I. Donskyi, K. Silberreis, L. Cuellar, J. Dernedde, G. Keil, T. C. Mettenleiter and R. Haag, *Macromol. Biosci.*, 2017, **17**, 1600499.
65 M. F. Gholami, D. Lauster, K. Ludwig, J. Storm, B. Ziem, N. Severin, C. Böttcher, J. P. Rabe, A. Herrmann and M. Adeli, *Adv. Funct. Mater.*, 2017, **27**, 1606477.
66 I. S. Donskyi, C. Nie, K. Ludwig, J. Trimpert, R. Ahmed, E. Quaas, K. Achazi, J. Radnik, M. Adeli and R. Haag, *Small*, 2021, **17**, 2007091.
67 E. Mohammadifar, V. Ahmadi, M. F. Gholami, A. Oehrl, O. Kolyvushko, C. Nie, I. S. Donskyi, S. Herziger, J. Radnik and K. Ludwig, *Adv. Funct. Mater.*, 2021, 2009003.
68 K. H. Tan, S. Sattari, I. S. Donskyi, J. L. Cuellar-Camacho, C. Cheng, K. Schwibbert, A. Lippitz, W. E. Unger, A. Gorbushina and M. Adeli, *Nanoscale*, 2018, **10**, 9525–9537.
69 B. Yu, J. Wang, X. Yang, W. Wang and X. Cai, *Environ. Sci. Pollut. Res.*, 2019, **26**, 32345–32359.
70 Z. Rezaeifar, Z. Es' haghi, G. H. Rounaghi and M. Chamsaz, *J. Chromatogr. B: Anal. Technol. Biomed. Life Sci.*, 2016, **1029**, 81–87.
71 Z. Rezaeifar, G. H. Rounaghi, Z. Es' haghi and M. Chamsaz, *Mater. Sci. Eng., C*, 2018, **91**, 10–18.
72 K. W. Lee, J. W. Chung and S.-Y. Kwak, *ACS Appl. Mater. Interfaces*, 2017, **9**, 33149–33158.
73 M. Adeli, R. Soleyman, Z. Beiranvand and F. Madani, *Chem. Soc. Rev.*, 2013, **42**, 5231–5256.
74 M. Adeli, N. Mirab, M. S. Alavidjeh, Z. Sobhani and F. Atyabi, *Polymer*, 2009, **50**, 3528–3536.
75 M. Adeli, N. Mirab and F. Zabihi, *Nanotechnology*, 2009, **20**, 485603.
76 L. Zhou, C. Gao and W. Xu, *Macromol. Chem. Phys.*, 2009, **210**, 1011–1018.
77 H. Huang, M. Liu, R. Jiang, J. Chen, Q. Huang, Y. Wen, J. Tian, N. Zhou, X. Zhang and Y. Wei, *Mater. Sci. Eng., C*, 2018, **91**, 458–465.
78 W. Wang and X. Cai, *Compos. Interfaces*, 2019, **26**, 989–1000.
79 F. Ernst, Z. Gao, R. Arenal, T. Heek, A. Setaro, R. Fernandez-Pacheco, R. Haag, L. Cognet and S. Reich, *J. Phys. Chem. C*, 2017, **121**, 18887–18891.
80 Y. Xia, S. Li, C. Nie, J. Zhang, S. Zhou, H. Yang, M. Li, W. Li, C. Cheng and R. Haag, *Appl. Mater. Today*, 2019, **16**, 518–528.
81 E. Castro, A. H. Garcia, G. Zavala and L. Echegoyen, *J. Mater. Chem. B*, 2017, **5**, 6523–6535.
82 M. Eskandari, A. Najdian and R. Soleyman, *Chem. Phys.*, 2016, **472**, 9–17.
83 Z. Beiranvand, A. Kakanejadifard, I. Donskyi, A. Faghani, Z. Tu, A. Lippitz, P. Sasanpour, F. Maschietto, B. Paulus and W. Unger, *RSC Adv.*, 2016, **6**, 112771–112775.
84 I. Donskyi, K. Achazi, V. Wycisk, C. Böttcher and M. Adeli, *Chem. Commun.*, 2016, **52**, 4373–4376.
85 I. S. Donskyi, K. Achazi, V. Wycisk, K. Licha, M. Adeli and R. Haag, *Langmuir*, 2017, **33**, 6595–6600.
86 N. Ebrahimi, R. Sadeghi, I. S. Donskyi and M. Adeli, *Fluid Phase Equilib.*, 2017, **450**, 57–64.
87 I. Donskyi, M. Drüke, K. Silberreis, D. Lauster, K. Ludwig, C. Kühne, W. Unger, C. Böttcher, A. Herrmann and J. Dernedde, *Small*, 2018, **14**, 1800189.
88 S. Sotoma and Y. Harada, *Langmuir*, 2019, **35**, 8357–8362.
89 T. Takimoto, T. Chano, S. Shimizu, H. Okabe, M. Ito, M. Morita, T. Kimura, T. Inubushi and N. Komatsu, *Chem. Mater.*, 2010, **22**, 3462–3471.
90 L. Zhao, T. Takimoto, M. Ito, N. Kitagawa, T. Kimura and N. Komatsu, *Angew. Chem., Int. Ed.*, 2011, **50**, 1388–1392.
91 Y. Zou, S. Ito, F. Yoshino, Y. Suzuki, L. Zhao and N. Komatsu, *ACS Nano*, 2020, **14**, 7216–7226.
92 Y. Zou and N. Komatsu, *Carbon*, 2020, **163**, 395–401.
93 L. Zhao, Y. H. Xu, H. Qin, S. Abe, T. Akasaka, T. Chano, F. Watari, T. Kimura, N. Komatsu and X. Chen, *Adv. Funct. Mater.*, 2014, **24**, 5348–5357.
94 L. Zhao, Y.-H. Xu, T. Akasaka, S. Abe, N. Komatsu, F. Watari and X. Chen, *Biomaterials*, 2014, **35**, 5393–5406.
95 T.-F. Li, K. Li, Q. Zhang, C. Wang, Y. Yue, Z. Chen, S.-J. Yuan, X. Liu, Y. Wen and M. Han, *Biomaterials*, 2018, **181**, 35–52.
96 T.-F. Li, Y.-H. Xu, K. Li, C. Wang, X. Liu, Y. Yue, Z. Chen, S.-J. Yuan, Y. Wen and Q. Zhang, *Acta Biomater.*, 2019, **86**, 381–394.
97 Z. Chen, S.-J. Yuan, K. Li, Q. Zhang, T.-F. Li, H.-C. An, H.-Z. Xu, Y. Yue, M. Han and Y.-H. Xu, *J. Controlled Release*, 2020, **320**, 469–483.
98 Z. Chen, C. Wang, T.-F. Li, K. Li, Y. Yue, X. Liu, H.-Z. Xu, Y. Wen, Q. Zhang and M. Han, *Nanomedicine*, 2019, **14**, 335–351.
99 S.-J. Yuan, Y.-H. Xu, C. Wang, H.-C. An, H.-Z. Xu, K. Li, N. Komatsu, L. Zhao and X. Chen, *J. Nanobiotechnol.*, 2019, **17**, 1–25.
100 F. Yoshino, T. Amano, Y. Zou, J. Xu, F. Kimura, Y. Furusho, T. Chano, T. Murakami, L. Zhao and N. Komatsu, *Small*, 2019, **15**, 1901930.
101 M. D. Torelli, A. G. Rickard, M. V. Backer, D. S. Filonov, N. A. Nunn, A. V. Kinev, J. M. Backer, G. M. Palmer and O. A. Shenderova, *Bioconjugate Chem.*, 2019, **30**, 604–613.
102 L. Zhao, Y. Nakae, H. Qin, T. Ito, T. Kimura, H. Kojima, L. Chan and N. Komatsu, *Beilstein J. Org. Chem.*, 2014, **10**, 707–713.

103 X. Li, L. Zhao, Q. Liang, J. Ye, N. Komatsu, Q. Zhang, W. Gao, M. Xu and X. Chen, *J. Biomed. Nanotechnol.*, 2017, **13**, 280–289.
104 H. Qin, K. Maruyama, T. Amano, T. Murakami and N. Komatsu, *Mater. Res. Express*, 2016, **3**, 105049.
105 L. Zhao, A. Shiino, H. Qin, T. Kimura and N. Komatsu, *J. Nanosci. Nanotechnol.*, 2015, **15**, 1076–1082.
106 L. M. Manus, D. J. Mastarone, E. A. Waters, X.-Q. Zhang, E. A. Schultz-Sikma, K. W. MacRenaris, D. Ho and T. J. Meade, *Nano Lett.*, 2010, **10**, 484–489.
107 W. Wang, Y. Zou, A. López-Moreno, Y. Jiang, F. Wen, H. X. Wang and N. Komatsu, *ChemNanoMat*, 2020, **6**, 1332–1336.
108 M. C. Lukowiak, B. Ziem, K. Achazi, G. Gunkel-Grabole, C. S. Popeney, B. N. Thota, C. Böttcher, A. Krueger, Z. Guan and R. Haag, *J. Mater. Chem. B*, 2015, **3**, 719–722.
109 H. Huang, M. Liu, R. Jiang, J. Chen, L. Mao, Y. Wen, J. Tian, N. Zhou, X. Zhang and Y. Wei, *J. Colloid Interface Sci.*, 2018, **513**, 198–204.
110 J. Boudou, M. David, V. Joshi, H. Eidi and P. Curmi, *Diamond Relat. Mater.*, 2013, **37**, 131–138.
111 N. Cai, C. Li, X. Luo, Y. Xue, L. Shen and F. Yu, *J. Mater. Sci.*, 2016, **51**, 797–808.
112 A. Li, X. Yang, B. Yu and X. Cai, *Res. Chem. Intermed.*, 2020, **46**, 101–118.
113 J. Zhou, H. Zhou, J. Tang, S. Deng, F. Yan, W. Li and M. Qu, *Microchim. Acta*, 2017, **184**, 343–368.
114 S. Li, Z. Guo, R. Feng, Y. Zhang, W. Xue and Z. Liu, *RSC Adv.*, 2017, **7**, 4975–4982.
115 X.-M. Zhang, X.-M. Wang, H.-L. Cong, Y.-Q. Shen and B. Yu, *Integr. Ferroelectr.*, 2019, **199**, 46–51.
116 Y. Wen, M. Xu, X. Liu, X. Jin, J. Kang, D. Xu, H. Sang, P. Gao, X. Chen and L. Zhao, *Colloids Surf., B*, 2019, **173**, 842–850.
117 X. Yang, A. Li, W. Wang, C. Zhang, J. Wang, B. Yu and X. Cai, *J. Chem. Technol. Biotechnol.*, 2018, **93**, 2635–2643.
118 S.-S. Yao, F.-L. Jin, K. Y. Rhee, D. Hui and S.-J. Park, *Composites, Part B*, 2018, **142**, 241–250.
119 B. Gao, Z. Hao, J. Zhang, R. Zhang and H. Cui, *ECS J. Solid State Sci. Technol.*, 2017, **6**, M89.
120 A. Daham, A. Zegaoui, H. A. Ghouti, M. Derradji, W.-a. Cai, J. Wang, W.-b. Liu, J.-y. Wang and Z. Moussa, *Compos. Interfaces*, 2020, **27**, 905–919.
121 B. Gao, J. Zhang, Z. Hao, L. Huo, R. Zhang and L. Shao, *Carbon*, 2017, **123**, 548–557.